MOL #30304

Real-time analysis of agonist-induced activation of protease-activated receptor 1 / $G_{\alpha i1}$ protein complex measured by BRET in living cells

Mohammed A. Ayoub, Damien Maurel, Virginie Binet, Michel Fink, Laurent Prézeau,

Hervé Ansanay and Jean-Philippe Pin.

CNRS UMR5203, Montpellier, F-34094 France; INSERM U661, Montpellier, F-34094 France; Université Montpellier I, Montpellier, F-34094 France; Université Montpellier II, Montpellier, F-34094 France. Institut de Génomique Fonctionnelle, Département de Pharmacologie Moléculaire, 141, rue de la Cardonille – 34094, Montpellier Cedex 5, France (MAA, DM, VB, LP, JPP).

CisBio International, BP 84175 – 30204, Bagnols-sur-Cèze Cedex, France (MF, HA).

1

MOL #30304

Running title: BRET analysis of PAR1 coupling to $G_{\alpha i1}$ protein

Corresponding author:

Jean-Philippe Pin, PhD. Institut de Génomique Fonctionnelle; Département de Pharmacologie Moléculaire; 141, rue de la Cardonille, Montpellier F-34094 Cedex 5, France.

Phone: **+33 467 14 2988 ;** Fax: **+33 467 54 2432** ; E-mail: **jppin@igf.cnrs.fr**

36 text pages

11 figures

0 table

46 references

Abstract: 250 words

Introduction: 697 words

Discussion: 1582 words

ABBREVIATIONS:

GPCRs, G protein-coupled receptors; PARs, protease-activated receptors; BRET, bioluminescence resonance energy transfer; FRET, fluorescence resonance energy transfer; Rluc, *Renilla* luciferase; YFP, yellow fluorescent protein; TRAP, thrombin receptor activating peptide; PTX, Pertussis toxin; cAMP, cyclic adenosine-3',5' monophosphate; GABAb, gamma 4-aminobutyric acid receptor type B; SRE, serum-response element; ELISA, Enzyme Linked ImmunoSorbent Assay.

2

MOL #30304

ABSTRACT

G protein-coupled receptors transmit extracellular signals into the cells by activating heterotrimeric G proteins, a process that is often followed by receptor desensitization. Monitoring such a process in real time and in living cells will help better understand how G protein activation occurs. Energy transfer-based approaches (FRET and BRET) were recently shown to be powerful methods to monitor GPCRs-G proteins association in living cells. Here, we used a BRET technique to monitor the coupling between the protease-activated receptor 1 (PAR1) and $G_{\alpha i1}$ protein. A specific constitutive BRET signal can be measured between non-activated PAR1 and the $G_{\alpha i1}$ protein expressed at physiological level. This signal is insensitive to Pertussis toxin (PTX) and likely reflects the pre-assembly of these two proteins. The BRET signal rapidly increases upon receptor activation in a PTX-sensitive manner. The BRET signal then returns to the basal level after few minutes. The desensitization of the BRET signal is concomitant with ß-arrestin-1 recruitment to the receptor, consistent with the known rapid desensitization of PARs. The agonist-induced BRET increase was dependent on the insertion site of fluorophores in proteins. Taken together, our results show that BRET between GPCRs and G_{α} proteins can be used to monitor the receptor activation in real time and in living cells. Our data also revealed that PAR1 can be part of a pre-assembled complex with $G_{\alpha i1}$ protein, resulting either from a direct interaction between these partners or from their co-localization in specific microdomains, and that receptor activation likely results in rearrangements within such complexes.

MOL #30304

INTRODUCTION

G protein-coupled receptors (GPCRs) represent one of the most important gene family in mammalian genomes. These receptors allow signals as diverse as photons, ions, amino acids, lipids, catecholamines, peptides or proteins to transmit information inside the cells by activating heterotrimeric G proteins formed by various α, β and γ subunits (Bockaert and Pin, 1999). However, the detailed analysis of GPCRs and G protein activation in living cells is still limited. Within the last few years, energy transfer technologies (FRET and BRET) were shown to enable such an analysis allowing to monitor the physical proximity between various partners of a GPCR signaling cascade: the receptor, G protein subunits and their effectors (Azpiazu and Gautam, 2004; Bunemann et al., 2003; Dowal et al., 2006; Frank et al., 2005; Galés et al., 2005; Galés et al., 2006; Hein et al., 2005; Janetopoulos et al., 2001; Nobles et al., 2005; Rebois et al., 2006; Yi et al., 2003). Agonist-promoted energy transfer changes has often been taken as the major indicator of either the association/dissociation of proteins or the transition from the inactive to active state of proteins. Indeed, while some authors linked the agonist-induced decrease of energy transfer signals with the reversible dissociation between G protein subunits (Azpiazu and Gautam, 2004; Janetopoulos et al., 2001; Yi et al., 2003), others proposed, in contrast, that no molecular dissociation occurred between α, β and γ subunits after receptor activation and the decrease in energy transfer signals reflects molecular rearrangements and conformational changes within the αβγ heterotrimer (Bunemann et al., 2003; Galés et al., 2006). Likewise, for the interaction between GPCRs and G proteins, some data are consistent with the association-dissociation model and the absence of receptor-G protein "*pre-association*" or "*pre-assembly*" (Hein et al., 2005), while others support a pre-assembly and agonist-induced conformational changes of pre-

assembled GPCRs-G proteins complexes (Galés et al., 2005; Galés et al., 2006; Nobles et al., 2005).

Protease-activated receptors (PARs) are a family of 4 different receptors that are activated by various proteases (Hollenberg and Compton, 2002; Macfarlane et al., 2001). PAR1, PAR3 and PAR4 respond to highly selective group of serine proteases that include thrombin, plasmin, the factor Xa and the activated protein C (Cottrell et al., 2002; Macfarlane et al., 2001). In contrast, PAR2 receptor can be activated by trypsin, tryptase and the coagulation factors VIIa and Xa (Macfarlane et al., 2001; Cottrell et al., 2002; Myatt and Hill, 2005). The activation mechanism of these receptors involved the cleavage of their N-terminal segment by the protease, unmasking a new N-terminus that acts as a tethered ligand, directly activating the transmembrane core of the receptor (Coughlin, 1999). Of interest, PARs can also be activated by synthetic peptides that mimic the tethered ligand, without the requirement of protease cleavage of receptors (Al-Ani et al., 2002; Chen et al., 1994; Vu et al., 1991). Such an activation mechanism leads to the constitutive activation of the receptor by proteases, followed by the rapid desensitization, internalization and degradation of the cleaved receptor (Chen et al., 2004; Cottrell et al., 2002; Trejo, 2003). This desensitization process involved the well characterized phosphorylation of the receptor by GRKs and the recruitment of arrestins (Paing et al., 2002; Trejo, 2003). PARs are involved in a number of physiological processes such as, thrombosis (Chung et al., 2002), vascular biology (Barnes et al., 2004), inflammation (Kannan, 2002) and the regulation of cell proliferation and tumorigenesis (Boire et al., 2005) and represent important new targets for the treatment of a number of pathologies.

In the present study, we used a BRET approach to monitor the coupling between PAR1 and $G_{\alpha i1}$ protein in living COS-7 cells. Our data show that PAR1 receptor activation

using either thrombin or agonist peptides mimicking the tethered ligands lead to a rapid, but transient, increase in the BRET signal measured between the receptor fused to YFP, and $G_{\alpha i1}$ fused to Rluc. The desensitization kinetic of this response is similar to that of the recruitment of ß-arrestin-1 to the receptor, indicating that the observed signal reflects the G protein activation in living cells. Of interest, our data also revealed a close proximity between the inactive receptor and the $G_{\alpha i1}$ protein consistent with their possible pre-assembly.

MOL #30304

MATERIAL AND METHODS

Materials: Human cDNAs for PAR1 and PAR2 were cloned into pcDNA3.1+ (Guthrie Research Institute, PA, USA); pcDNA3-Rluc, Rluc-ß-arrestin-1, V2-YFP and $G_{\alpha i1}$-122-Rluc were generously provided by R. Jockers, M. G. Scott (Institut Cochin, Paris, France), T. Durroux (IGF, Montpellier, France), C. Galés and M. Bouvier (Université de Montréal, Canada), respectively; bovine thrombin (~93 NIH units/mg protein, 1 unit/ml ≈ 0.3 µM) and bovine trypsin pancreas (Calbiochem, Merck KgaA, Darmstadt, Germany); mouse anti-PAR1 antibody (Zymed Laboratories, San Francisco, CA); monoclonal anti-Flag M2 (Sigma-Aldrich, St. Louis, MO); the polyclonal rabbit anti-$G_{\alpha i1/2}$ antibody (Lledo et al., 1992) and TRAP-14 peptide (Ser-Phe-Leu-Leu-Arg-Asn-Pro-Asn-Asp-Lys-Tyr-Glu-Pro-Phe-NH2) were a generous gift of Dr. V. Homburger (IGF, Montpellier, France); SCH79797 compound (N-3-cyclopropyl-7-{[4-(1-methyl-ethyl)phenyl]methyl}-7H-pyrrolo[3,2-f]quinazoline-1,3 diamine); TFLLR (Thr-Phe-Leu-Leu-Arg-NH2) and SLIGRL (Ser-Leu-Iso-Gly-Arg-Leu-NH2) peptides (Tocris, Ellisville, MO, USA); 96-well white microplates (Greiner Bio-One SAS, Courtaboeuf, France); Coelenterazine h substrate (Promega, Charbonnières, France).

Plasmid constructions: PAR1-YFP and PAR2-YFP fusion proteins were obtained by fusing the cDNA coding for YFP (yellow fluorescent protein) at the C-terminal end of receptors. For this, the coding regions of the human PARs have been amplified without stop codon using forward and reverse primers bearing the cloning BamHI site. The PCR products were inserted in phase between BamHI site into pRK6-YFP plasmid (T. Durroux, IGF, Montpellier). Similar strategy has been followed for the truncation of the N-terminus (PAR1-ΔN-YFP) and the deletion of the C-terminus (PAR1-ΔC-YFP) of PAR1 using the BamHI cloning site. For

7

all these constructs, the junction sequence between PARs and YFP was similar coding for ten residues (YRDPRVPVAT).

For $G_{\alpha i1}$-Rluc fusion protein, site-directed mutagenesis was first performed on the cDNA of the human $G_{\alpha i1}$ to insert an EcoRI site between position encoding isoleucine 93 and aspartic acid 94 within the helical domain of the G protein (see Fig.11C). Then, the intermediate construct ($G_{\alpha i1}$-EcoRI) was used to insert at the EcoRI site the coding region of the *Renilla* luciferase enzyme (Rluc) without stop codon and bearing the glycine rich-linker sequences coding for Gly-Asn-Ser-Gly-Gly in the 5' end and Gly-Gly-Gly-Asn-Ser in the 3' end, respectively. The PCR product of Rluc was inserted in phase between EcoRI site of $G_{\alpha i1}$-EcoRI plasmid. For $G_{\alpha s}$-Rluc construct, the fusion was performed between alanine 188 and aspartic acid 189 using NheI site with glycine rich-linker similar to that used for $G_{\alpha i1}$-Rluc. For Flag-PAR1-YFP construct, the MluI/HindIII fragment of PAR1-YFP obtained by PCR was inserted between MluI and HindIII into pRK5-Flag-GABAb1 containing the mGluR5 signal peptide to allow its expression and targeting to the cell surface. All constructs were verified by sequencing and their expression in COS-7 cells was confirmed by luminescence, fluorescence and western blot.

Cell culture and transfection*:* COS-7 cells were grown in complete medium (DMEM supplemented with 10 % (v/v) FBS, 4.5 g/l glucose, 100 U/ml penicillin, 0.1 mg/ml streptomycin, 1 mM glutamine)(all from Life Technologies (Gaithersburg, MD)). Transient transfections were performed using electroporation as described previously (Brabet et al., 1998).

Microplate BRET assay and Kinetics analysis*:* twenty-four hours post-transfection, COS-7 cells were detached with PBS and 5 mM EDTA, washed three times with PBS and

resuspended in a suitable volume of PBS. Cells at a density of $2\text{-}5.10^4$ cells per well were distributed in a 96-well microplate. Coelenterazine h substrate was added at a final concentration of 5 µM in the total volume of 50 µl per well. Readings were then immediately performed after the addition of different ligands at room temperature and at 0.05 or 0.5 s intervals and during several minutes using the Mithras LB 940 plate reader (Berthold Biotechnologies, Bad Wildbad, Germany) that allows the sequential integration of light signals detected with two filter settings (Rluc filter: 485 ± 20 nm and YFP filter: 530 ± 25 nm). For the kinetic studies, we have used the injection system of the Mithras reader. Data were collected using the MicroWin2000 software (Berthold Biotechnologies) and BRET signal was expressed in milliBRET units of BRET ratio as previously described (Ayoub et al., 2002). For dose-response data, curves were fitted with a nonlinear regression and sigmoid dose-response equation using GraphPad Prism software.

The kinetics analysis of the ligand-induced BRET signal between $G_{\alpha i1}$-Rluc and PAR1-YFP was performed on two time windows. The activation kinetic was determined on a time window of 50 s after thrombin injection (window 1) corresponding to a phase during which the desensitization process was reduced. Similarly, the desensitization kinetic was determined on a time window from 5 to 15 min after thrombin injection (window 2). For the activation kinetics, the signal was fitted with GraphPad Prism Software using the equation: $Y = Plateau + (Top_{window1} - Plateau)*(1-exp^{(-k*(X-X0))})$, in which $Top_{window1}$ corresponds to the maximal BRET signal reached after thrombin injection and X_0 is the time of thrombin injection. For the desensitization kinetics, the signal was fitted using the equation: $Y = (Top_{window2} - Bottom)*(1-exp^{-k*X}) + Bottom$, in which $Top_{window2}$ corresponds to the BRET signal reached after 5 min of thrombin injection. For both equations, X is the time, plateau represents the basal BRET before thrombin injection and bottom represents the mean BRET signal after 15 min. The halftime value ($t_{1/2}$) was calculated as the ratio 0.69/k.

For the kinetic of ß-arrestin-1 translocation, thrombin-promoted BRET signal was fitted using the equation: $Y = Top*(1-exp^{(-k*X)})$, in which Top corresponds to the maximal BRET signal and X is the time.

cAMP assay: The determination of the cAMP accumulation in COS-7 cells was performed in 96-wells microplates using the HTRF®-cAMP Dynamic kit (CisBio International, Bagnols sur Cèze, France). Briefly, cells were stimulated 30 minutes at 37°C with ligands in the presence or the absence of 10 µM forskolin in 50 mM phosphate buffer, pH 7.0, 0.2% BSA, 0.02% NaN_3 and preservatives. The reaction was stopped by 50 mM phosphate buffer, pH 7.0, 1 M KF and 1% Triton X-100 containing HTRF® assay reagents: the Europium Cryptate-labeled anti-cAMP antibody and the XL-665-labeled cAMP. The assay was incubated overnight at 4°C and TR-FRET signal were measured 50 µs after excitation at 620 nm and 665 nm using a RubyStar instrument (BMG Labtechnologies, Champigny-sur-Marne, France).

Inositol phosphate measurements: The determination of the inositol phosphate 1 accumulation in COS-7 cells was performed in 96-wells microplates using the HTRF®-IP-One kit (CisBio International). Briefly, cells were stimulated 30 minutes at 37°C with thrombin in the stimulation buffer pH 7.4: HEPES 10 mM, $CaCl_2$ 1 mM, $MgCl_2$ 0.5 mM, KCl 4.2 mM, NaCl 146 mM, glucose 5.5 mM, LiCl 50 mM pH 7.4. The reaction was stopped by 50 mM phosphate buffer, pH 7.0, 1 M KF and 1% Triton X-100 containing HTRF® assay reagents: the Europium Cryptate-labeled anti-IP1 antibody and d2-labeled IP1. The assay was incubated overnight at 4°C and TR-FRET signal were measured 50 µs after excitation at 620 nm and 665 nm using a RubyStar instrument.

MOL #30304

ELISA: Twenty-four hours post-transfection, COS-7 cells were fixed 5 minutes at room temperature with 4% of paraformaldehyde and permeabilized or not 5 minutes with 0.05% Triton X-100. Cells were then blocked with phosphate-buffered saline containing 1% fetal calf serum, incubated 30 minutes at room temperature with 1 µg/ml of monoclonal anti-PAR1 or anti-Flag M2 antibodies. After washing steps, cells were incubated 30 minutes with 0.5 µg/ml of HRP-coupled anti-mouse secondary antibody (Amersham Pharmacia) and washed again. Bound antibody was detected using a SuperSignal substrate (Pierce, Rockford, IL) and a Mithras LB 940 plate reader.

Luciferase gene reporter assay: COS-7 cells were transfected with the serum-response element-luciferase gene reporter (SRE-Luc) and PAR1 receptors, washed with PBS and switched to serum-free DMEM overnight. Cells were then treated or not with ligands for six hours in the serum-free DMEM at 37°C, washed with PBS and lysed with the reagent containing the luciferase substrate (Promega Bright-Glo™ Luciferase Assay System). Luminescence was measured immediately using the Mithras LB 940 instrument.

Ligand Binding Assay: Ligand binding assay was performed as previously described (Galvez et al., 2001) with 40000 cells/well and using the radiolabled GABAb receptor antagonist, [^{3}H]-CGP54626 (specific activity = 40 Ci/mmol) at the final concentration of 5 nM. Specific binding was determined by the incubation of cells with GABA 1 mM and the number of receptors per well or per cell was determined and correlated with the ELISA signal using the anti-Flag antibody.

Western blotting: COS-7 cells transfected or not with $G_{\alpha i1}$ or $G_{\alpha i1}$–Rluc were lysed in Laemmli buffer (125 mM Tris–HCl, pH 6.8, 4% sodium dodecyl sulfate (SDS), 20%

11

glycerol, 0.01% bromophenol blue) and warmed 5 minutes at 90°C. Samples were then resolved by 10% SDS-polyacrylamide gel electrophoresis, transferred to nitrocellulose membrane (Amersham Pharmacia) and subjected to immunoblotting using a polyclonal rabbit anti-$G_{\alpha i1/2}$ antibody (Lledo et al., 1992). Immunoreactive bands were visualized by the ECL detection Kit (Amersham Pharmacia) on Kodak ML light films.

Confocal imaging: COS-7 cells transiently expressing PAR1-YFP were fixed 5 minutes at room temperature with 4% of paraformaldehyde and washed with PBS. Cover slips were then mounted with Gel/Mount (Biomeda, Foster City, CA) and microscopic observations were performed on an Leica SP2 UV confocal microscope with a Plan-Apochromat 63x/1.4 oil objective with the appropriate YFP spectrums sittings.

Statistical analysis: Two-way ANOVA test associated to Bonferroni post-test (GraphPad Prism software) was used to determine statistically significant differences between control (in the absence of ligands) and stimulated conditions.

MOL #30304

RESULTS

Protease-activated receptor type 1 (PAR1) and G$_{\alpha i1}$ protein fused to energy acceptor and donor proteins. To monitor the coupling of PAR1 to G$_{\alpha i1}$ protein using a BRET approach, these two proteins were fused with the energy acceptor yellow fluorescent protein (YFP) and the energy donor luciferase from *Renilla reniformis* (Rluc), respectively (Fig. 1A). The YFP was fused at the C-terminus of PAR1 and this did not alter its expression at the cell surface as shown by confocal microscopy (Fig. 1B) or ELISA assay with the anti-PAR1 antibody (Fig. 1C) showing that the majority of receptors is expressed on the cell surface. Functional analysis showed that PAR1-YFP activated signaling pathways in similar way than the wild-type receptor, as monitored by the inositol phosphate production (Fig. 1D), luciferase gene reporter and cAMP assays (data not shown). Thrombin potency measured on cells expressing PAR1-YFP (EC$_{50}$ = 1 ± 0.4 nM, n=3) was similar to that measured on cell expressing PAR1 (EC$_{50}$ = 1.68 ± 1.3 nM, n=3).

The G$_{\alpha i1}$-Rluc was obtained by inserting Rluc within the helical domain of the G$_{\alpha i1}$ protein between Ile 93 and Asp 94 residues. Such a position was chosen based on the crystal structure of the G$\alpha\beta\gamma$ heterotrimeric complex, and was already used in many other studies with either G$_{\alpha i}$ (Bunemann et al., 2003; Frank et al., 2005; Galés et al., 2006), G$_{\alpha s}$ (Hynes et al., 2004; Yi et al., 2003) or G$_{\alpha o}$ (Azpiazu and Gautam, 2004; Nobles et al., 2005). In all cases, these fusion G proteins were shown to be correctly expressed and to allow an efficient coupling of receptors to their effectors. Indeed, like G$_{\alpha i1}$ (~ 43 kDa) our G$_{\alpha i1}$-Rluc is correctly expressed at the expected molecular weight (~ 78 kDa) as shown by western blot using the antibody that recognizes G$_{\alpha i1}$ as well as G$_{\alpha i2}$ subunits (Fig. 1E) and by luminescence measurements (Fig. 2C). Note that the G$_{\alpha i1}$-Rluc expression level is close to that of the

13

endogenous proteins. The functionality of $G_{\alpha i1}$-Rluc construct is illustrated by its ability to potentiate the inhibition of forskolin-stimulated cAMP production mediated by PAR1-YFP in a PTX-sensitive manner (Fig. 1F). In addition, the co-expression of $G_{\alpha i1}$-Rluc with PAR1-YFP (Fig. 1G), lysophosphatidic acid or GABAb (data not shown) receptors largely enhanced agonist-induced inhibition of cAMP production. Such a potentiation in cAMP inhibition did not result from an increased expression level of PAR1 at the cell surface in the presence of the co-transfected $G_{\alpha i1}$ protein, as shown using an ELISA assay performed on intact cells using anti-PAR1 antibody (data not shown).

Monitoring PAR1-$G_{\alpha i1}$ proximity in living cells by BRET. In cells co-expressing PAR1-YFP and $G_{\alpha i1}$-Rluc, a significant basal BRET signal was detected compared to cells co-expressing $G_{\alpha s}$-Rluc and PAR1-YFP or V2-YFP (Fig. 2A and B). When cells were treated with thrombin (50 U/ml ≈ 15 µM), the BRET signal significantly increased between PAR1-YFP and $G_{\alpha i1}$-Rluc but not $G_{\alpha s}$-Rluc (Fig. 2A). In contrast, the BRET between $G_{\alpha s}$-Rluc and V2-YFP can be specifically increased after cell stimulation with vasopressin (1 µM) (Fig. 2B). These differences in the basal BRET signal and the sensitivity to receptor activation between $G_{\alpha i1}$-Rluc and $G_{\alpha s}$-Rluc were not due to the difference in the expression level of BRET partners quantified by luminescence and fluorescence measurements (Fig. 2C). These results are compatible with the coupling properties of PAR1 and V2 receptors illustrated in Fig. 1F, since PAR1 is known to activate $G_{\alpha i1}$ but not $G_{\alpha s}$ and inversely for V2.

The specificity of the basal and the protease-induced BRET signal. To demonstrate the specificity of both the basal and agonist-induced BRET signal, we performed BRET-saturation assay previously developed to demonstrate the specificity of protein-protein interactions (Ayoub et al., 2004; Mercier et al., 2002). Indeed, when the amount of $G_{\alpha i1}$-Rluc

was maintained constant, increasing the amount of PAR1-YFP leads to an increase in the BRET ratio that reaches a plateau (Fig. 3A). This plateau likely corresponds to the situation where all $G_{\alpha i1}$-Rluc proteins available are specifically "pre-assembled" with available PAR1-YFP. Of interest, activation of the receptor leads to an increase in the maximal saturated BRET, consistent with a change in the energy transfer efficiency, rather than to the recruitment of additional G proteins in the vicinity of the receptor.

The specificity of the energy transfer was also verified by the BRET-competition assay (Ayoub et al., 2002). The constitutive and thrombin-promoted BRET signals between PAR1-YFP and "non-saturating" amount of $G_{\alpha i1}$-Rluc can be decreased by the co-expression of the untagged $G_{\alpha i1}$ protein (Fig. 3B). This was not due to the change in the acceptor/donor (YFP/Rluc) ratio controlled by measuring both luminescence (Rluc signal) and fluorescence (YFP signal) signals (Fig. 3C). This further confirms that the amount of $G_{\alpha i1}$ proteins in the vicinity of the receptor is saturable.

Quantification of PAR1 expression at the cell surface. To determine the number of PAR1 receptors at the cell surface, we used a Flag-PAR1-YFP construct that possesses a Flag epitope inserted at the N-terminus. This receptor was shown to share the same functional properties as the wild-type PAR1 in terms of its ability to activate the inositol phosphate formation (data not shown). ELISA assay revealed that the receptor is correctly targeted to the cell surface (Fig. 4A). By comparing the ELISA signal with Flag-PAR1-YFP with that measured with a Flag-GABAb receptor for which the exact expression level can be determined by binding studies on intact cells with a non-permeable radioligand (Fig. 4B), we calculated an expression of about 100,000 Flag-PAR1-YFP receptors per COS-7 cell. Fluorescence measurements indicate that Flag-PAR1-YFP receptor expression is 5 times

lower than the PAR1-YFP under similar transfection conditions (Fig. 4C), such that the

measured basal BRET between Flag-PAR1-YFP and $G_{\alpha i1}$-Rluc is also lower (Fig. 4D), but

still within the BRET saturation curve as indicated by the corresponding YFP/Rluc ratio (Fig.

3A).

Real-time analysis of PAR1-$G_{\alpha i1}$ association and desensitization. Kinetic analysis showed

that thrombin-induced BRET increase between $G_{\alpha i1}$-Rluc and PAR1-YFP occurred rapidly

($t_{1/2} = 4.3 \pm 0.6$ s, n=13) (Fig. 5A). This increase persists few minutes and returns to the basal

signal 15 minutes after protease application (Fig. 5B), consistent with known PAR1

desensitization properties (Trejo, 2003). Indeed, when the signal was measured after pre-

incubation 30 minutes with thrombin, no BRET increase was observed (Fig. 5C). Of interest,

this decrease in agonist-induced BRET is concomitant with the recruitment of ß-arrestin1 to

PAR1 also monitored by BRET. Indeed, thrombin application induced a BRET increase

between Rluc-ß-arrestin-1 and PAR1-YFP in a dose-dependent manner with a potency (EC_{50}

$= 2 \pm 0.3$ nM, n=3) similar to that determined in other functional assays (Fig. 6A). Moreover,

kinetic analysis shows that $t_{1/2}$ value of the recruitment of ß-arrestin-1 (5.4 ± 0.9 min, n=5)

(Fig. 6B) is compatible with that of the decay phase of agonist-induced BRET between $G_{\alpha i1}$-

Rluc and PAR1-YFP ($t_{1/2} = 6.9 \pm 1.7$ min, n=8, assuming a mono-exponential decay) (Fig.

5B). These data demonstrate that a fast and reversible process is involved in the increase in

BRET between PAR1 and $G_{\alpha i1}$ resulting from receptor activation and the

activation/desensitization processes of PAR1 can be studied by BRET.

PARs activation is responsible for the increase in the BRET signal. Several lines of

evidence indicate that thrombin-induced BRET increase results from PAR1 activation. First,

when using a trypsin-activated PAR2 receptor (Coughlin, 2000; Macfarlane et al., 2001) fused

to YFP instead of PAR1, a similar basal BRET was measured with $G_{\alpha i1}$-Rluc that is increased

16

MOL #30304

after trypsin (100 nM) but not thrombin stimulation (Fig. 7A). Second, thrombin (Fig. 7B)

and trypsin (Fig. 7C) effects on PAR1 and PAR2, respectively, were dose-dependent with

EC_{50} values (6.3 ± 0.2 nM, n=17 and 1.3 ± 0.3 nM, n=3, respectively) comparable to

potencies reported for these proteases on PARs (Al-Ani et al., 2002; Boire et al., 2005;

O'Brien et al., 2000). Third, peptides known to mimic the activating N-terminal end of PARs

after their cleavage by proteases increased the BRET signal. This was obtained either with the

non-selective PAR-activating peptide TRAP-14 (100 µM)(Debeir et al., 1996) or with the

PAR1-selective (TFLLR, 100 µM)(Chung et al., 2002) agonist peptides on PAR1 expressing

cells (Fig. 8A). The PAR2-selective peptide (SLIGRL, 100 µM)(Al-Ani et al., 2002) had no

effect on PAR1 expressing cells (Fig. 8A) but it was active on PAR2 expressing cells (data

not shown). The TFLLR-induced BRET increase was dose-dependent with an EC_{50} value of

5.8 ± 1.9 µM (n=8) in agreement with its reported potency on PAR1 (Fig. 8B) (Seeley et al.,

2003). Like for thrombin, kinetics analysis shows that peptide-induced BRET increase occurs

rapidly ($t_{1/2}$ = 6.5 ± 1.5 s, n=5) (Fig. 8C). Similar effect of the PAR1-selective peptide was

observed when PAR1 was deleted of its N-terminal end containing the tethered ligand (PAR1-

ΔN-YFP) (Fig. 8D) and making the receptor insensitive to thrombin (Fig. 8E and F).

Finally, both protease inhibitors (Fig. 9A) and the PAR1 selective non-peptidic antagonist

SCH79797 (10 µM) (Fig. 9B) completely abolished the agonist-promoted BRET increase

without affecting the basal BRET signal.

Agonist-induced BRET increase is associated to $G_{\alpha i1}$ activation. We next examined

whether the basal and agonist-induced BRET result from G protein activation. Inactivating

$G_{\alpha i1}$-Rluc with Pertussis toxin (PTX, 100 ng/ml) (Fig. 10) suppressed agonist-induced BRET,

but not the basal signal. This demonstrates that the basal BRET measured in the absence of

PAR1 activation does not results from G protein activation. Moreover, these data reveal that

17

the mode of interaction or assembly between $G_{\alpha i1}$ and PAR1 (the distance and/or the relative orientation of Rluc and YFP fused to $G_{\alpha i1}$ and PAR1, respectively) is likely different whether the receptor is in its inactive or active state.

Movement within the pre-assembled PAR1-$G_{\alpha i1}$ complexes represents the major cause of the agonist-induced BRET increase. To get more insights in the molecular events leading to BRET increase after receptor activation, similar experiments were conducted with a receptor in which the YFP was inserted at a different site, closer to the helix 8 (PAR1-ΔC-YFP)(Fig. 11A). Indeed, if the increase in BRET resulting from receptor activation is due to the recruitment of additional $G_{\alpha i1}$ protein in the close vicinity of the receptor, this should be observed whatever the YFP position on the receptor. Such a deletion completely abolished the agonist-induced recruitment of ß-arrestin1 but not its ability to activate G proteins (data not shown). A high basal BRET signal was measured between PAR1-ΔC-YFP and $G_{\alpha i1}$-Rluc, but the activation of this mutant with either thrombin or TFLLR did not lead to any change in the BRET signal (Fig. 11B).

We also examined the influence of the Rluc position in $G_{\alpha i1}$ protein on the basal and agonist-induced BRET. For this reason, we used a $G_{\alpha i1}$ fusion protein in which Rluc was inserted at position Ala121-Glu122 in the helical-rich domain ($G_{\alpha i1}$-122-Rluc)(Galés et al., 2006). In this construct, the Rluc is positioned on the other side of the G protein compared to $G_{\alpha i1}$-Rluc used so far in our study (Fig. 11C). As shown in Fig. 11D, a larger basal BRET is observed with both PAR1-YFP and PAR1-ΔC-YFP and $G_{\alpha i1}$-122-Rluc compared to $G_{\alpha i1}$-Rluc (Fig. 11B), and this despite a similar expression level of all partners (data not shown). However, no further increase in BRET was observed upon activation of the receptors with either thrombin or TFLLR (Fig. 11D). Taken together, these data clearly dissociate the BRET increase from the recruitment of the G protein by the activated receptor and support the

proposal that PAR1 and $G_{\alpha i1}$ are pre-assembled, and that receptor activation lead to a change

in the positioning of the $G_{\alpha i1}$ subunit relative to the receptor.

DISCUSSION

The application of energy transfer-based assays to study the interaction between GPCRs and their cognate G proteins constitutes an attractive field of research in GPCRs biology. Here, we monitored the physical proximity between PAR1 and $G_{\alpha i1}$ protein using a BRET approach in living COS-7 cells. Our data show that the kinetic of BRET changes resulting from PAR1 receptor activation is consistent with the fast activation process, and the known desensitization properties of these receptors. These data further indicate that BRET signals measured between the receptor and G protein can be used to monitor GPCRs activation and desensitization in real time and in living cells.

Our data first revealed a significant basal BRET signal between PARs-YFP (PAR1 and PAR2) and $G_{\alpha i1}$-Rluc. This basal BRET is specific since it was not observed with $G_{\alpha s}$-Rluc, in agreement with the known coupling properties of PARs (Coughlin, 2000; Macfarlane et al., 2001), and is saturable as shown by the BRET-saturation experiment and the displacement by the "unlabeled" $G_{\alpha i1}$ protein. Moreover, such a basal BRET is measured with $G_{\alpha i1}$-Rluc expression level similar to that of endogenous $G_{\alpha i1}$, and is observed for receptor expression level at the cell surface of about 100,000 receptors per COS-7 cell. This is consistent with the known physiological expression of PAR1 in platelets (about 1,000 receptors per platelet (Brass et al., 1992; Norton et al., 1993), corresponding to 100,000 receptors per COS-7 cell assuming the later is 10 times larger in diameter).

Recent studies using BRET or FRET approaches also reported a constitutive energy transfer between GPCRs and G proteins (Azpiazu and Gautam, 2004; Bunemann et al., 2003; Frank et al., 2005; Galés et al., 2005; Galés et al., 2006; Hein et al., 2005; Janetopoulos et al., 2001; Nobles et al., 2005; Yi et al., 2003). The authors propose that this is due either to the existence of a "*pre-associated*" or "*pre-assembled*" receptor-G protein complexes, or to the

constitutive activity of the GPCR. Our data do not support that the basal BRET signal results from any possible constitutive activation of $G_{\alpha i1}$ by PARs. Indeed, there is so far no evidence for the constitutive activity of PARs including in our expression system (data not shown). Moreover, the basal BRET is not inhibited by PAR1 antagonist and PTX did not affect the basal BRET, whereas it clearly prevents the agonist-induced increase in BRET. This firmly demonstrates that the basal BRET does not result from the activation of $G_{\alpha i1}$.

An increasing number of recent publications using BRET or FRET techniques reported the study of the physical proximity between various partners of a GPCR signaling cascade: the receptor, G proteins and their effectors (Azpiazu and Gautam, 2004; Bunemann et al., 2003; Dowal et al., 2006; Frank et al., 2005; Galés et al., 2005; Galés et al., 2006; Hein et al., 2005; Janetopoulos et al., 2001; Nobles et al., 2005; Rebois et al., 2006; Yi et al., 2003). Such a close proximity suggests a direct interaction between these partners. However, despite major efforts we have not been able to observe co-immunoprecipitation of PARs and $G_{\alpha i1}$ protein. Although the direct interaction between PARs and $G_{\alpha i1}$ is a likely explanation, our data may also well be explained by a co-localization of both partners in specific small microdomains. Indeed, recent studies using single-molecule tracking reported that GPCR diffusion is restricted to small microdomains that may be limited by specific fences under the plasma membrane (Kusumi et al., 2005; Suzuki et al., 2005), or may possibly correspond to caveolae or lipid raft (Insel et al., 2005; Meyer et al., 2006). If the G proteins are also incorporated into such microdomains, this will likely result in a limited number of G proteins in the close vicinity of the receptor, consistent with a saturable basal BRET signal observed. Moreover, the likely high density of both receptors and G proteins in such microdomains (Insel et al., 2005) may favor energy transfer between Rluc and YFP fused to these partners. Other recent study by BRET and bimolecular fluorescence complementation approaches reported that receptors and G proteins complexes are formed early during proteins

biosynthesis (Dupre et al., 2006), such that part of the basal BRET observed likely reflect such pre-formed intracellular complexes. However, we would like to point out that the basal BRET cannot result solely from intracellular complexes, as demonstrated by the BRET saturation experiment shown in Fig. 3A. The proportion of intracellular receptors is expected to increase when receptor expression levels reach saturation. If the basal BRET only reflects intracellular complexes, then the basal BRET value relative to the agonist-induced BRET value should largely increase with receptor expression. This is clearly not the case.

Our second main observation is that PAR1 activation using either thrombin or peptides mimicking the tethered ligand leads to a rapid increase in the BRET signal measured between the receptor and $G_{\alpha i1}$. These effects were specific of the receptor-protease/peptide pair. Moreover, the BRET increase was completely prevented by protease inhibitors, PAR1 antagonist and PTX indicating that agonist-induced BRET increase reflects the activation of receptor-G protein complexes. The agonist-induced BRET increase between $G_{\alpha i1}$-Rluc and PAR1-YFP was found to be rapid, in agreement with the rapid activation of G proteins by other GPCRs (Bunemann et al., 2003; Galés et al., 2005; Galés et al., 2006) and consistent with what is expected for such a process. Our kinetic analysis revealed a $t_{1/2}$ of about 5 seconds when using saturating concentrations of thrombin, a process that appears slower than that reported for $G_{\alpha i}$ activation by the α_2-adrenergic receptor using either BRET (Galés et al., 2005; Galés et al., 2006) or FRET (Hein et al., 2005). This may well result from differences in the activation kinetic between different GPCRs, as observed between the PTH and α_2-adrenergic receptors (Vilardaga et al., 2003).

Further evidence that ligand-induced BRET increase results from G protein activation comes from the reversibility of this effect, consistent with the well known PAR1 receptor desensitization (Trejo, 2003). Indeed, our data revealed that the agonist-induced BRET was largely decreased after 10 minutes and disappeared after 30 minutes, a kinetic that

nicely fits with that of thrombin-induced β-arrestin-1 recruitment also monitored by BRET.

This data clearly indicates that agonist-induced BRET increase, but not the basal signal, is

associated to PAR1 and $G_{\alpha i1}$ protein activation and further confirms the role of ß-arrestin-1 in

G protein uncoupling and PAR1 desensitization.

Two possibilities can explain the increase in BRET ratio observed between PARs

and $G_{\alpha i1}$ protein after activation: 1) additional recruitment of $G_{\alpha i1}$ protein by the active form of

the receptor or 2) a change in the relative positioning of the fused YFP and Rluc within the

pre-assembled receptors and G proteins. Our data are not consistent with the additional

recruitment of $G_{\alpha i1}$ proteins in the pre-assembled complexes. Indeed, when increasing the

amount of PAR1-YFP fusion protein with a constant amount of $G_{\alpha i1}$-Rluc, a saturation limit

in the basal BRET signal is observed suggesting that all receptors are pre-assembled with the

G protein under these conditions. Upon receptor activation, this maximal BRET value is

increased. This is consistent with a better efficacy in the energy transfer within the pre-

assembled receptor-G protein complex after activation, rather than an increase in the number

of G proteins interacting with the receptor. Accordingly, the increase in BRET signal

observed after receptor activation likely results from a relative movement of the fused Rluc

and YFP in the pre-assembled complexes. This proposal is also supported by the differential

sensitivity to PTX treatment of the basal and agonist-induced BRET. Because a direct

interaction between the C-terminal tail of $G_{\alpha i1}$ protein (the target of PTX), and the second and

third intracellular loops of the receptor is known to occur during activation (Bourne, 1997),

this further indicates that $G_{\alpha i1}$ and PAR1 interacts in a specific manner with the active form of

the receptor. Moreover, the movement hypothesis is supported by the fact that the agonist-

induced BRET change largely depends on the relative positioning of the Rluc and YFP in the

G protein and the receptor, respectively. Indeed, the agonist-induced BRET increase is

completely abolished when the YFP is fused closer to the helix 8 of PAR1 (in agreement with

the expected movement of the C-terminal tail of the receptor during activation) (Fig. 11B), and is not observed if Rluc is inserted on the other side of the $G_{\alpha i1}$ protein (Fig. 11C and D). This would not be expected if the increase in BRET simply results from G protein recruitment in the vicinity of the activated receptor.

Taken together, our data are consistent with a pre-assembly between $G_{\alpha i1}$ protein and PARs, and their relative movement occurring after receptor activation. Whether such a pre-assembly results from a direct interaction of PARs and the G protein, or their co-localization in small and saturable membrane microdomains remains to be further studied. Whatever, this is compatible with recent studies reporting the existence of pre-assembled complexes between receptors, G proteins and effectors (Galés et al., 2005; Nobles et al., 2005; Galés et al., 2006; Rebois et al., 2006; Dowal et al., 2006). All these studies proposed that energy transfer changes reflect conformational changes within the pre-associated complexes rather than receptor activation-promoted association. This suggests that the assembly of GPCRs, G proteins and effectors does not represent a limiting step in the activation process and further documents the hypothesis that these partners can be part of pre-assembled protein complexes responsible for GPCRs-mediated signaling, offering the way to a higher selectivity and a faster process.

MOL #30304

REFERENCES

Al-Ani B, Wijesuriya SJ and Hollenberg MD (2002) Proteinase-activated receptor 2: differential activation of the receptor by tethered ligand and soluble peptide analogs. *J Pharmacol Exp Ther* **302**:1046-54.

Ayoub MA, Couturier C, Lucas-Meunier E, Angers S, Fossier P, Bouvier M and Jockers R (2002) Monitoring of ligand-independent dimerization and ligand-induced conformational changes of melatonin receptors in living cells by bioluminescence resonance energy transfer. *J Biol Chem* **277**:21522-8.

Ayoub MA, Levoye A, Delagrange P and Jockers R (2004) Preferential formation of MT1/MT2 melatonin receptor heterodimers with distinct ligand interaction properties compared with MT2 homodimers. *Mol Pharmacol* **66**:312-21.

Azpiazu I and Gautam N (2004) A fluorescence resonance energy transfer-based sensor indicates that receptor access to a G protein is unrestricted in a living mammalian cell. *J Biol Chem* **279**:27709-18.

Barnes JA, Singh S and Gomes AV (2004) Protease activated receptors in cardiovascular function and disease. *Mol Cell Biochem* **263**:227-39.

Bockaert J and Pin JP (1999) Molecular tinkering of G protein-coupled receptors: an evolutionary success. *Embo J* **18**:1723-9.

Boire A, Covic L, Agarwal A, Jacques S, Sherifi S and Kuliopulos A (2005) PAR1 Is a Matrix Metalloprotease-1 Receptor that Promotes Invasion and Tumorigenesis of Breast Cancer Cells. *Cell* **120**:303-13.

Bourne HR (1997) How receptors talk to trimeric G proteins. *Curr Opin Cell Biol* **9**:134-42.

Brabet I, Parmentier ML, De Colle C, Bockaert J, Acher F and Pin JP (1998) Comparative effect of L-CCG-I, DCG-IV and gamma-carboxy-L-glutamate on all cloned metabotropic glutamate receptor subtypes. *Neuropharmacology* **37**:1043-51.

Brass LF, Vassallo RR, Jr., Belmonte E, Ahuja M, Cichowski K and Hoxie JA (1992) Structure and function of the human platelet thrombin receptor. Studies using monoclonal antibodies directed against a defined domain within the receptor N terminus. *J Biol Chem.* **267**:13795-8.

Bunemann M, Frank M and Lohse MJ (2003) Gi protein activation in intact cells involves subunit rearrangement rather than dissociation. *Proc Natl Acad Sci U S A* **100**:16077-82.

Chen CH, Paing MM and Trejo J (2004) Termination of protease-activated receptor-1 signaling by beta-arrestins is independent of receptor phosphorylation. *J Biol Chem* **279**:10020-31.

Chen J, Ishii M, Wang L, Ishii K and Coughlin SR (1994) Thrombin receptor activation. Confirmation of the intramolecular tethered liganding hypothesis and discovery of an alternative intermolecular liganding mode. *J Biol Chem* **269**:16041-5.

Chung AW, Jurasz P, Hollenberg MD and Radomski MW (2002) Mechanisms of action of proteinase-activated receptor agonists on human platelets. *Br J Pharmacol* **135**:1123-32.

Cottrell GS, Coelho AM and Bunnett NW (2002) Protease-activated receptors: the role of cell-surface proteolysis in signalling. *Essays Biochem* **38**:169-83.

Coughlin SR (1999) How the protease thrombin talks to cells. *Proc Natl Acad Sci U S A* **96**:11023-7.

Coughlin SR (2000) Thrombin signalling and protease-activated receptors. *Nature* **407**:258-64.

Debeir T, Benavides J and Vige X (1996) Dual effects of thrombin and a 14-amino acid peptide agonist of the thrombin receptor on septal cholinergic neurons. *Brain Res* **708**:159-66.

Dowal L, Provitera P and Scarlata S (2006) Stable association between Galpha (q) and phospholipase Cbeta 1 in living cells. *J Biol Chem* **281**:23999-4014.

Dupre DJ, Robitaille M, Ethier N, Villeneuve LR, Mamarbachi AM and Hebert TE (2006) Seven transmembrane receptor core signaling complexes are assembled prior to plasma membrane trafficking. *J Biol Chem* **281**:34561-73.

Frank M, Thumer L, Lohse MJ and Bunemann M (2005) G Protein Activation without Subunit Dissociation Depends on a G{alpha}i-specific Region. *J Biol Chem* **280**:24584-90.

Galés C, Rebois RV, Hogue M, Trieu P, Breit A, Hébert TE and Bouvier M (2005) Real-time monitoring of receptor and G-protein interactions in living cells. *Nature Methods* **2**:177-184.

Galés C, Van Durm JJ, Schaak S, Pontier S, Percherancier Y, Audet M, Paris H and Bouvier M (2006) Probing the activation-promoted structural rearrangements in preassembled receptor-G protein complexes. *Nat Struct Mol Biol* **13**:778-86.

Galvez T, Duthey B, Kniazeff J, Blahos J, Rovelli G, Bettler B, Prezeau L and Pin JP (2001) Allosteric interactions between GB1 and GB2 subunits are required for optimal GABA(B) receptor function. *Embo J.* **20**:2152-9.

Hein P, Frank M, Hoffmann C, Lohse MJ and Bunemann M (2005) Dynamics of receptor/G protein coupling in living cells. *Embo J* **24**:4106-14.

Hollenberg MD and Compton JS (2002) International Union of Pharmacology. XXVIII. Proteinase-Activated Receptors. *Pharmacological Reviews* **54**:203-217.

Hynes TR, Mervine SM, Yost EA, Sabo JL and Berlot CH (2004) Live cell imaging of Gs and the beta2-adrenergic receptor demonstrates that both alphas and beta1gamma7 internalize upon stimulation and exhibit similar trafficking patterns that differ from that of the beta2-adrenergic receptor. *J Biol Chem* **279**:44101-12.

Insel PA, Head BP, Patel HH, Roth DM, Bundey RA and Swaney JS (2005) Compartmentation of G-protein-coupled receptors and their signalling components in lipid rafts and caveolae. *Biochem Soc Trans.* **33**:1131-4.

Janetopoulos C, Jin T and Devreotes P (2001) Receptor-mediated activation of heterotrimeric G-proteins in living cells. *Science* **291**:2408-11.

Kannan S (2002) Role of protease-activated receptors in neutrophil degranulation. *Med Hypotheses* **59**:266-7.

Kusumi A, Nakada C, Ritchie K, Murase K, Suzuki K, Murakoshi H, Kasai RS, Kondo J and Fujiwara T (2005) Paradigm shift of the plasma membrane concept from the two-dimensional continuum fluid to the partitioned fluid: high-speed single-molecule tracking of membrane molecules. *Annu Rev Biophys Biomol Struct.* **34**:351-78.

Lledo PM, Homburger V, Bockaert J and Vincent JD (1992) Differential G protein-mediated coupling of D2 dopamine receptors to K+ and Ca2+ currents in rat anterior pituitary cells. *Neuron.* **8**:455-63.

Macfarlane SR, Seatter MJ, Kanke T, Hunter GD and Plevin R (2001) Proteinase-Activated Receptors. *Pharmacological Reviews* **53**:245-282.

Mercier JF, Salahpour A, Angers S, Breit A and Bouvier M (2002) Quantitative assessment of beta 1- and beta 2-adrenergic receptor homo- and heterodimerization by bioluminescence resonance energy transfer. *J Biol Chem.* **277**:44925-31 Epub 2002 Sep 19.

Meyer BH, Segura JM, Martinez KL, Hovius R, George N, Johnsson K and Vogel H (2006) FRET imaging reveals that functional neurokinin-1 receptors are monomeric and

reside in membrane microdomains of live cells. *Proc Natl Acad Sci U S A.* **103**:2138-43 Epub 2006 Feb 3.

Nobles M, Benians A and Tinker A (2005) Heterotrimeric G proteins precouple with G protein-coupled receptors in living cells. *Proc Natl Acad Sci U S A* **102**:18706-11.

Norton KJ, Scarborough RM, Kutok JL, Escobedo MA, Nannizzi L and Coller BS (1993) Immunologic analysis of the cloned platelet thrombin receptor activation mechanism: evidence supporting receptor cleavage, release of the N-terminal peptide, and insertion of the tethered ligand into a protected environment. *Blood.* **82**:2125-36.

O'Brien PJ, Prevost N, Molino M, Hollinger MK, Woolkalis MJ, Woulfe DS and Brass LF (2000) Thrombin responses in human endothelial cells. Contributions from receptors other than PAR1 include the transactivation of PAR2 by thrombin-cleaved PAR1. *J Biol Chem.* **275**:13502-9.

Paing MM, Stutts AB, Kohout TA, Lefkowitz RJ and Trejo J (2002) beta -Arrestins regulate protease-activated receptor-1 desensitization but not internalization or Down-regulation. *J Biol Chem.* **277**:1292-300 Epub 2001 Nov 2.

Rebois RV, Robitaille M, Gales C, Dupre DJ, Baragli A, Trieu P, Ethier N, Bouvier M and Hebert TE (2006) Heterotrimeric G proteins form stable complexes with adenylyl cyclase and Kir3.1 channels in living cells. *J Cell Sci.* **119**:2807-18.

Seeley S, Covic L, Jacques SL, Sudmeier J, Baleja JD and Kuliopulos A (2003) Structural basis for thrombin activation of a protease-activated receptor: inhibition of intramolecular ligading. *Chem Biol* **10**:1033-41.

Suzuki K, Ritchie K, Kajikawa E, Fujiwara T and Kusumi A (2005) Rapid hop diffusion of a G-protein-coupled receptor in the plasma membrane as revealed by single-molecule techniques. *Biophys J.* **88**:3659-80 Epub 2005 Jan 28.

Trejo J (2003) Protease-activated receptors: new concepts in regulation of G protein-coupled receptor signaling and trafficking. *J Pharmacol Exp Ther* **307**:437-42.

Vilardaga JP, Bunemann M, Krasel C, Castro M and Lohse MJ (2003) Measurement of the millisecond activation switch of G protein-coupled receptors in living cells. *Nat Biotechnol* **21**:807-12.

Vu TK, Hung DT, Wheaton VI and Coughlin SR (1991) Molecular cloning of a functional thrombin receptor reveals a novel proteolytic mechanism of receptor activation. *Cell* **64**:1057-68.

Yi TM, Kitano H and Simon MI (2003) A quantitative characterization of the yeast heterotrimeric G protein cycle. *Proc Natl Acad Sci U S A* **100**:10764-9.

MOL #30304

FOOTNOTES

ADDRESS FOR REPRINT REQUESTS

Jean-Philippe Pin, PhD; Institut de Génomique Fonctionnelle ; Département de Pharmacologie Moléculaire ; 141, rue de la Cardonille, Montpellier F-34094 Cedex 5, France.

Phone: **+33 467 14 2988 ;** Fax: **+33 467 54 2432** ; E-mail: **jppin@igf.cnrs.fr**

MOL #30304

FIGURE LEGENDS

Figure 1: Cell expression and functional analysis of PAR1-YFP and $G_{\alpha i1}$-Rluc fusion proteins. A) For BRET experiments, PAR1 and G_α proteins ($G_{\alpha i1}$ and $G_{\alpha s}$) were fused to the yellow fluorescent protein (YFP) and *Renilla* luciferase (Rluc), respectively and transiently co-expressed in COS-7 cells as described in "Material and Methods" section. B) Confocal microscopy on COS-7 cells transiently expressing PAR1-YFP. C) ELISA assay performed on cells expressing or not PAR1-YFP and permeabilized or not with Triton X-100 (0.05%) using the monoclonal anti-PAR1 antibody (1 µg/ml). D) Inositol phosphate 1 production measured on cells expressing or not either PAR1 or PAR1-YFP and stimulated with increasing concentrations of thrombin. E) Western blotting on cells expressing or not $G_{\alpha i1}$ or $G_{\alpha i1}$-Rluc (3 µg of DNA each) using the anti-$G_{\alpha i1/2}$ antibody (1:1000)(*NS, non-specific band*). F) Ligand-promoted intracellular cAMP modulation in cells expressing PAR1-YFP or V2-YFP in the absence or presence of either $G_{\alpha i1}$-Rluc or $G_{\alpha s}$-Rluc. The treatment with Pertussis toxin (PTX, 100 ng/ml) was performed overnight at 37°C before the cells stimulation and cAMP measurements. G) Thrombin-promoted intracellular cAMP modulation in cells expressing PAR1-YFP in the absence or presence of $G_{\alpha i1}$-Rluc fusion protein. For cAMP assay, data represent the percentage of inhibition of forskolin-induced cAMP production. Data are representative of three independent experiments. ***, $p < 0.001$. **, $p < 0.01$; compared to control (in the absence of ligand).

Figure 2: Specific constitutive and thrombin-promoted BRET between PAR1 and $G_{\alpha i1}$ protein in living COS-7 cells. BRET measurements were performed on cells co-expressing $G_{\alpha i1}$-Rluc or $G_{\alpha s}$-Rluc with either PAR1-YFP (A) or V2-YFP (B) in the absence or presence of thrombin (50 U/ml ~ 15 µM) or AVP (1 µM) as indicated. E) Quantification of the

luciferase (Rluc) activity (□) and YFP fluorescence (■) of BRET partners measured in BRET-assay. Data are representative of three independent experiments. ***, $p < 0.001$. **, $p < 0.01$; compared to control (in the absence of ligand).

Figure 3: BRET-saturation and BRET-competition assays of the BRET between PAR1 and $G_{\alpha i1}$. A) BRET-saturation assay was performed on cells co-expressing constant amount of $G_{\alpha i1}$-Rluc fusion protein (energy donor) and increasing amounts of PAR1-YFP (energy acceptor) and BRET signal was determined in the absence (□) or presence (▲) of thrombin (50 U/ml) and fitted with fluorescence/luminescence ratio (YFP/Rluc) using a nonlinear regression equation (GraphPad Prism software). The arrow indicates the Flag-PAR1-YFP/$G_{\alpha i1}$-Rluc ratio (~ 0.04) for which the receptor number has been determined by radiobinding assay and corresponding to 100,000 Flag-PAR1-YFP receptors/cell (see Fig. 4). B) BRET-competition assay was performed on cells transiently co-expressing $G_{\alpha i1}$-Rluc and PAR1-YFP with an excess of the untagged $G_{\alpha i1}$ protein and in the absence (□) or presence (■) of thrombin. C) Quantification of the luciferase (Rluc) activity (□) and YFP fluorescence (■) measured in BRET-competition assay. The saturation curve represents the mean ± S.E.M of three individual experiments and data shown in panels B and C are representative of three independents experiments. ***, $p < 0.001$. *, $p < 0.05$; compared to control (in the absence of thrombin) or to pRK6 (in the absence of the untagged $G_{\alpha i1}$).

Figure 4: Quantification of PAR1 expression at the cell surface. A) ELISA assay were performed on intact and permeabilized cells transiently expressing the indicated receptors using the anti-Flag antibody (1 µg/ml). B) Correlation between the ELISA signal with Flag-GABAb receptor measured on non-permeabilized cells and the receptor number determined by radiobinding assay as described in "Material and Methods" section and represented as

fmoles of receptors/well or receptor number/cell. Cells transiently expressing $G_{\alpha i1}$-Rluc and either PAR1-YFP or Flag-PAR1-YFP were used to determine the relative expression level of $G_{\alpha i1}$-Rluc by luminescence (□) and receptors by fluorescence (■)(C) and to measure the energy transfer between the G protein and receptors in the absence or presence of thrombin (50 U/ml). Data are representative of at least 3 independent experiments. ***, $p < 0.001$; compared to control (in the absence of thrombin).

Figure 5: Kinetic analysis of thrombin-induced BRET increase between PAR1 and $G_{\alpha i1}$. Cells transiently co-expressing $G_{\alpha i1}$-Rluc and PAR1-YFP were used for BRET experiments and repetitive signals were recorded immediately before and after the injection of thrombin (50 U/ml) during 125 seconds (A) or 15 minutes (B). For the panel A, BRET signal was fitted as described in "Material and Methods" section. C) Cells transiently co-expressing $G_{\alpha i1}$-Rluc and PAR1-YFP were pre-treated or not with thrombin 30 minutes at 37°C and BRET measurements were then performed immediately after stimulation (■) or not (□) with thrombin. Data are representative of 13 (A), 8 (B) and 3 (C) independent experiments. ***, $p < 0.001$; compared to control (in the absence of thrombin).

Figure 6: Thrombin-induced ß-arrestin1 recruitment to PAR1 monitored by BRET. For BRET experiments on COS-7 cells transiently expressing Rluc-ß-arrestin-1 and PAR1-YFP, cells were pre-treated either 30 minutes at 37°C with increasing concentrations of thrombin (A) or with (50 U/ml ~ 15 µM) of thrombin at the indicated time (B). For the panel B, the kinetic analysis is described in "Material and Methods" section. Data are representative of 3 (A) or 5 (B) independent experiments.

Figure 7: The BRET increase is receptor- and protease-specific. A) The $G_{\alpha i1}$-Rluc fusion protein was transiently co-expressed with PAR1-YFP or PAR2-YFP as indicated and energy transfer measurements were performed at 25°C immediately after stimulation or not with thrombin (50 U/ml) or trypsin (100 nM). Dose-response experiments of thrombin- (B) or trypsin- (C) induced BRET increase between $G_{\alpha i1}$ protein and PARs as indicated. Data are mean ± S.E.M of 6 (A), 17 (B) or 3 (C) independent experiments. ***, $p < 0.001$. ns, $p > 0.05$; compared to control (in the absence of ligands).

Figure 8: Thrombin-induced BRET increase can be mimicked by PARs peptides. A) Cells transiently co-expressing $G_{\alpha i1}$-Rluc and PAR1-YFP were used for BRET experiments after the rapid stimulation with thrombin (50 U/ml) or peptides (TFLLR, TRAP-14, SLIGRL)(100 µM) as indicated. B) Dose-response of TFLLR-induced BRET increase. C) Kinetics analysis of TFLLR-induced BRET increase between $G_{\alpha i1}$-Rluc and PAR1-YFP. D) Schematic sequence PAR1-ΔN-YFP mutant in which the thrombin cleavage site and the tethered ligand were deleted. E) Luciferase gene reporter assay were performed on cells transfected with the SRE-Luc plasmid with either PAR1-YFP or PAR1-ΔN-YFP and treated 6 hours at 37°C with thrombin (50 U/ml) or the TFLLR peptide (100 µM) as indicated. F) BRET measurements on cells transiently co-expressing $G_{\alpha i1}$-Rluc and PAR1-ΔN-YFP in the absence or presence of thrombin (50 U/ml) or the TFLLR peptide (100 µM) as indicated. Data are the mean ± S.E.M of 3 (A) or 8 (B) independent experiments. For panels C), E) and F), data are representative of 5, 3 and 3 independent experiments, respectively. ***, $p < 0.001$. ns, $p > 0.05$; compared to control (in the absence of ligands).

Figure 9: Agonist-induced BRET increase is associated with the receptor activation. BRET measurements were performed in the absence or presence of thrombin or the TFLLR

peptide on cells transiently co-expressing $G_{\alpha i1}$-Rluc and PAR1-YFP and pre-treated or not 15 minutes at room temperature with a mixture of protease inhibitors (A) or 3 hours at 37°C with the PAR1-selective antagonist SCH79797 (10 µM)(B). Data are representative of 3 independent experiments. ***, $p < 0.001$. **, $p < 0.01$; compared to control (in the absence of ligands).
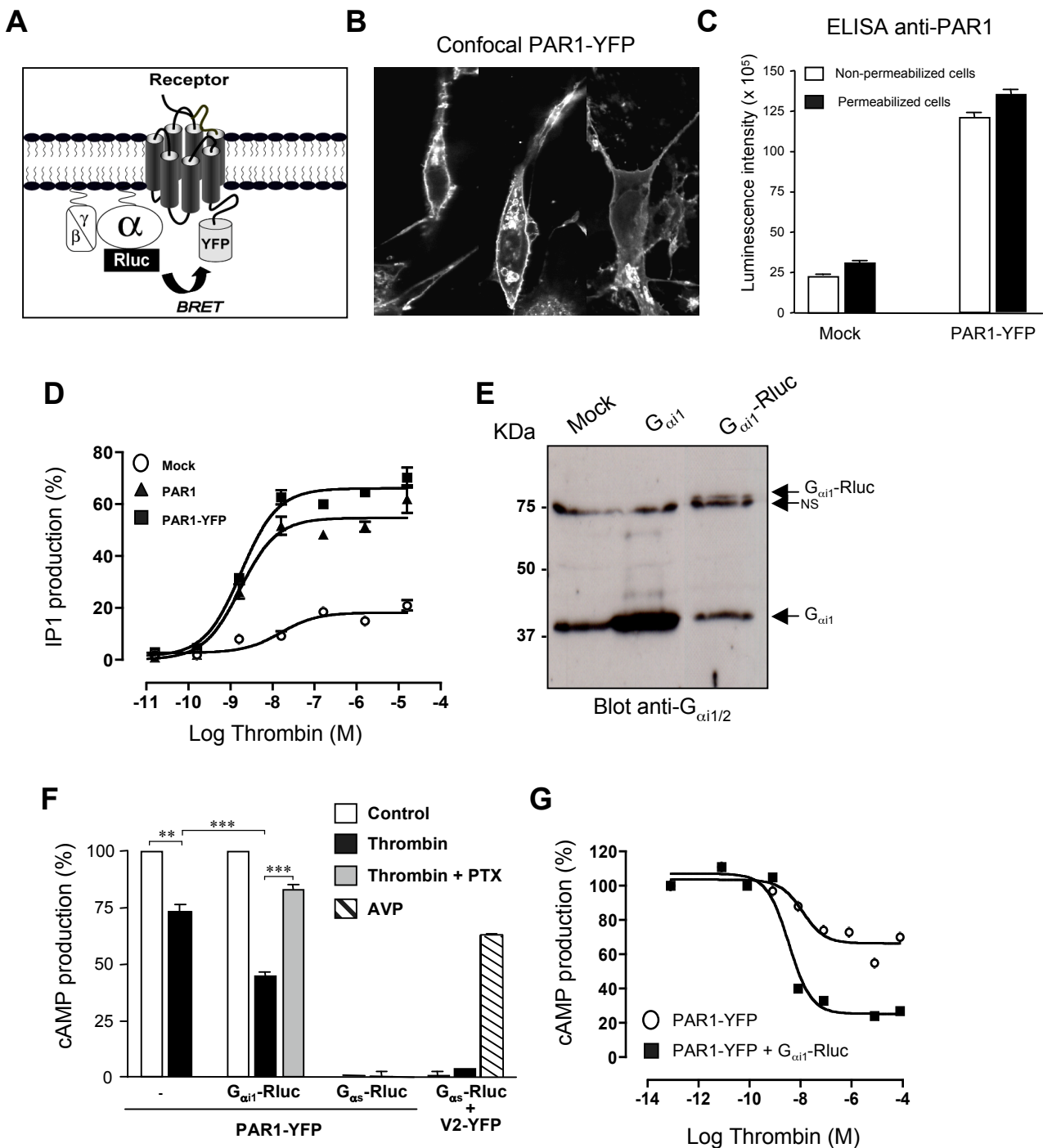
Figure 10: Agonist-induced BRET increase is associated with $G_{\alpha i1}$ protein activation. BRET measurements were performed in the absence or presence of thrombin or the TFLLR peptide on cells transiently co-expressing $G_{\alpha i1}$-Rluc and PAR1-YFP and pre-treated or not overnight at 37°C with Pertussis toxin (100 ng/ml). Data are representative of 3 independent experiments. ***, $p < 0.001$. ns, $p > 0.05$; compared to control (in the absence of ligands or PTX).

Figure 11: The BRET increase depends on the position of Rluc and YFP within the pre-assembled PAR1-$G_{\alpha i1}$ complexes. A) Schematic sequence of the YFP fusion protein of the C-terminus-deleted PAR1 (PAR1-ΔC-YFP). BRET measurements were than performed in the absence or presence of thrombin or the TFLLR peptide on cells transiently co-expressing $G_{\alpha i1}$-Rluc (B) or $G_{\alpha i1}$-122-Rluc (D) with either PAR1-YFP or PAR1-ΔC-YFP as indicated. C) Structural representation of the $G_{\alpha i1}$-GDP subunit (**PDB code 1GP2**) indicating the insertion sites of Rluc within the helical domain of the G protein. Data are representative of 3 independent experiments. ***, $p < 0.001$; compared to control (in the absence of ligands).

Figure 1

Figure 2

A

B

C
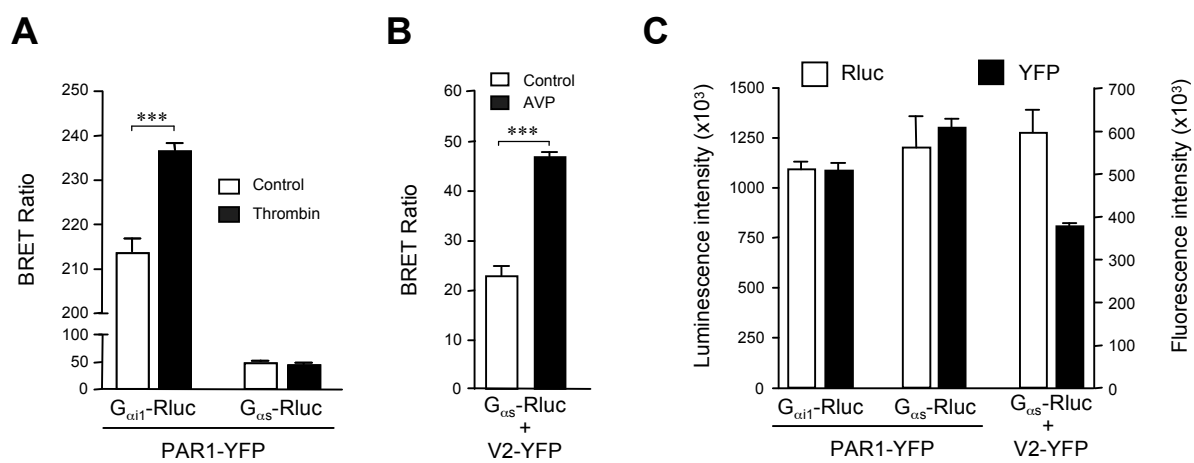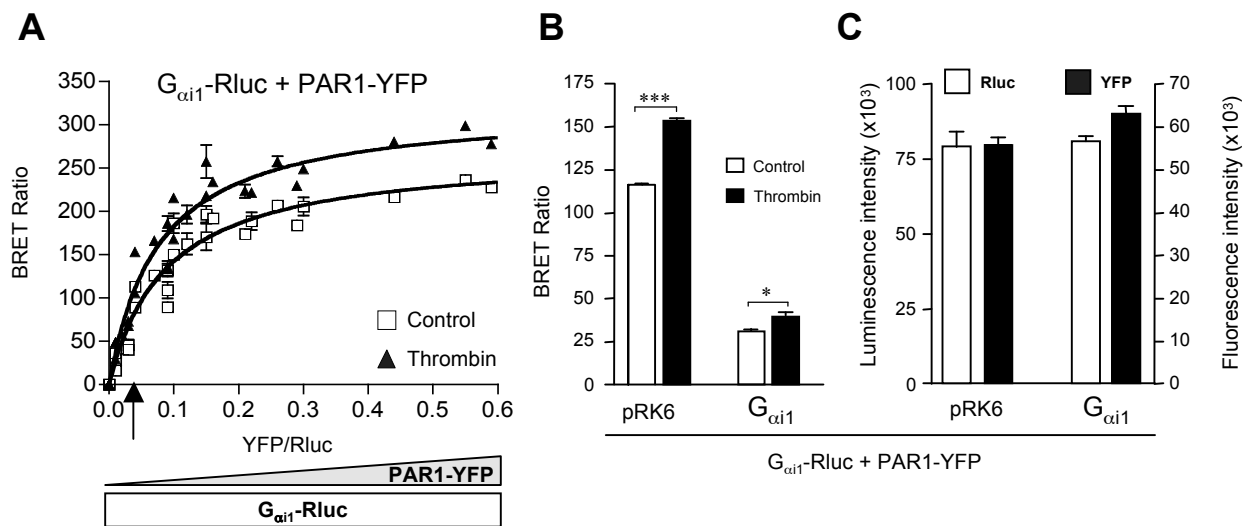
Figure 3

Figure 4

MOL #30304

Figure 5

Figure 6

A Rluc-ß-arrestin-1 + PAR1-YFP

B Rluc-ß-arrestin-1 + PAR1-YFP

Figure 7

MOL #30304

A — Control, Thrombin, Trypsin. BRET Ratio vs PAR1-YFP and PAR2-YFP ($G_{\alpha i1}$-Rluc)

B — $G_{\alpha i1}$-Rluc + PAR1-YFP. BRET (% of control) vs Log [Thrombin] (M)

C — $G_{\alpha i1}$-Rluc + PAR2-YFP. BRET (% of control) vs Log [Trypsin] (M)
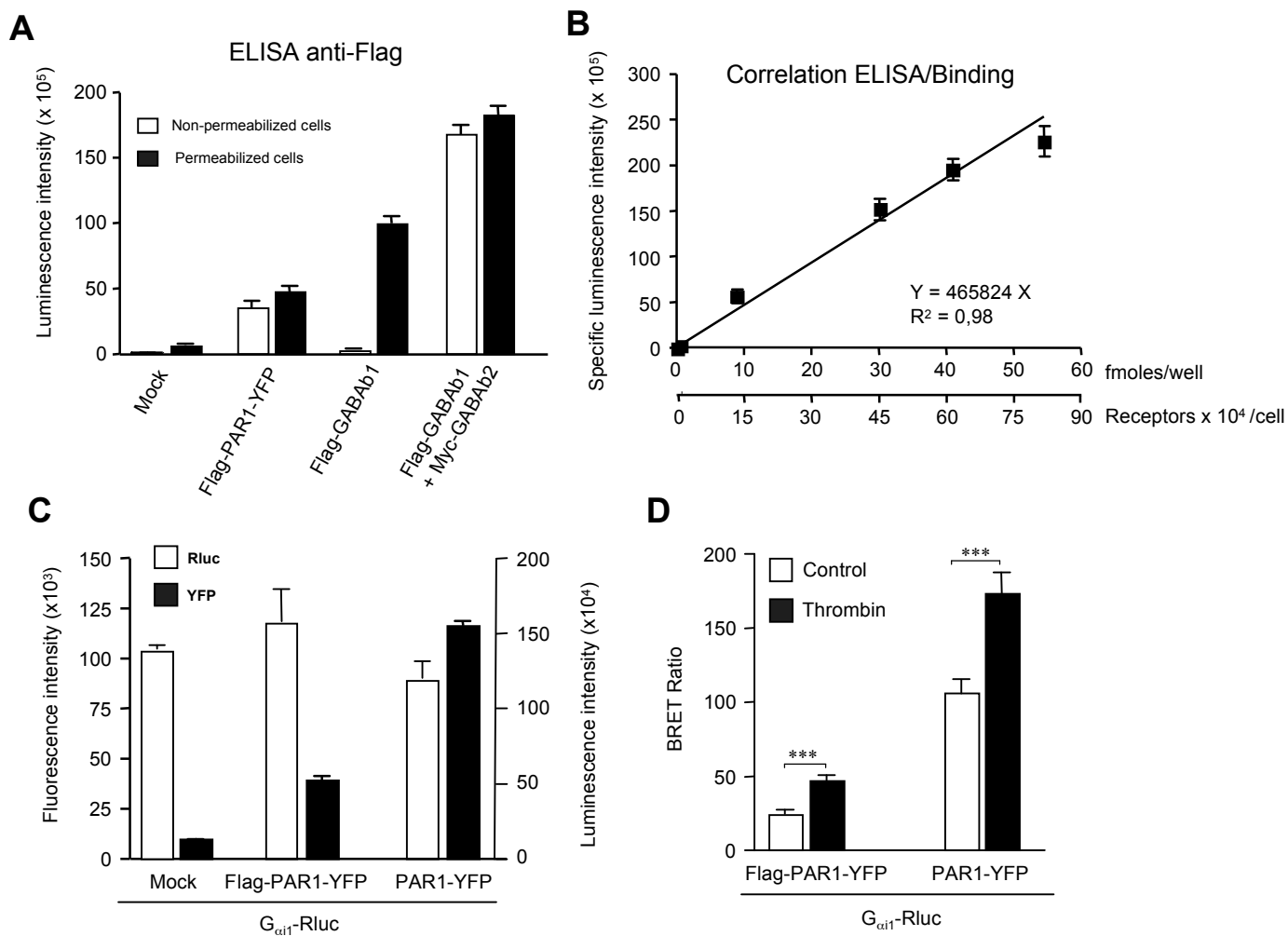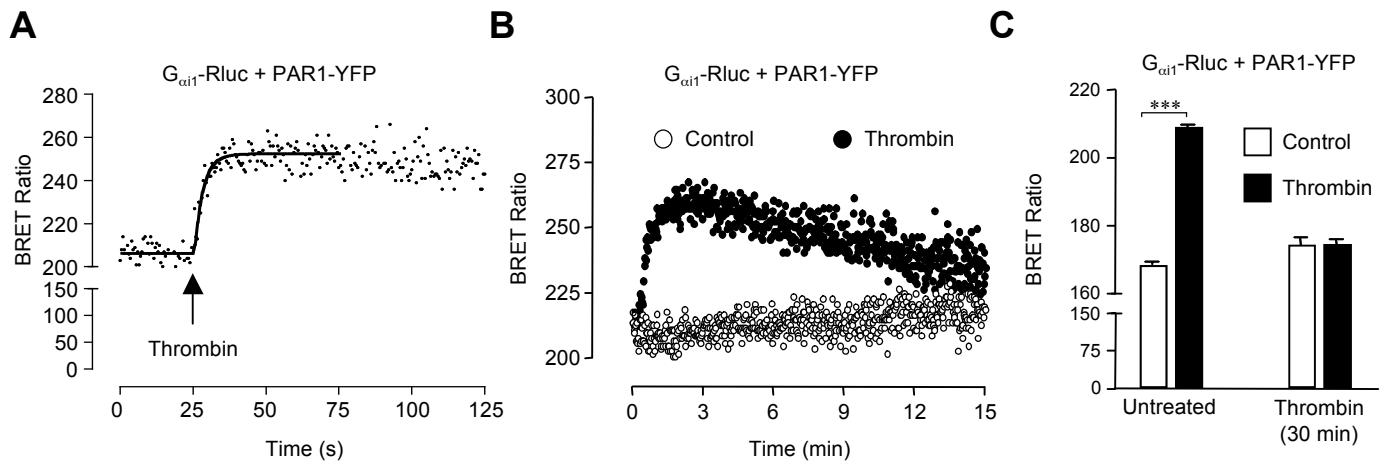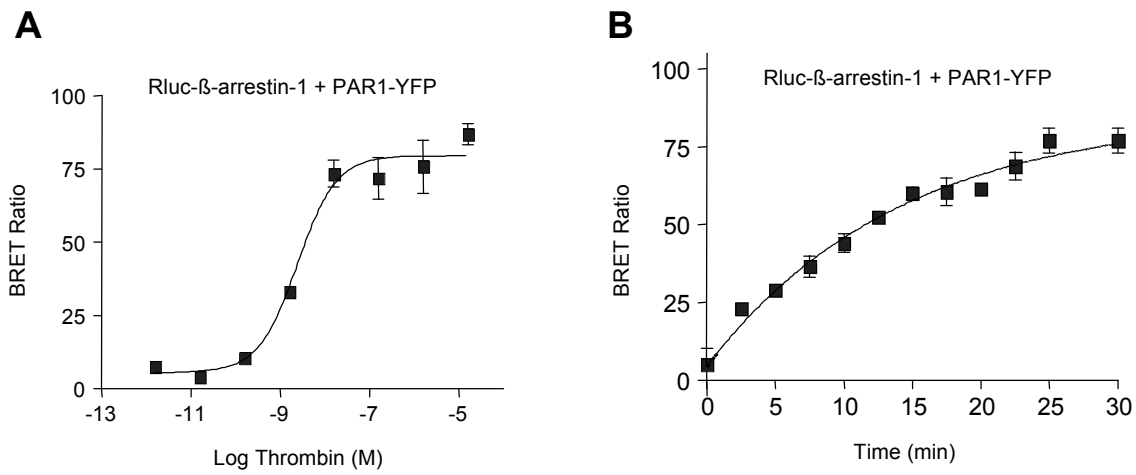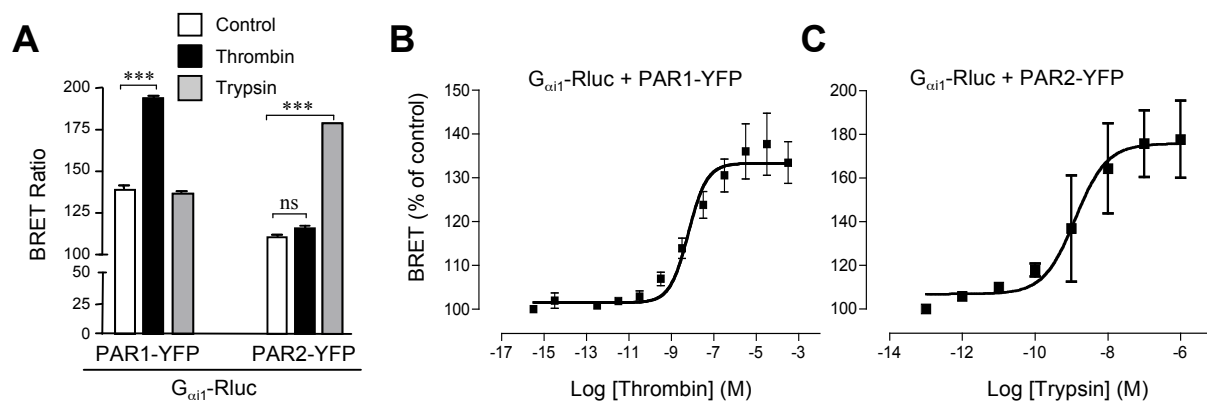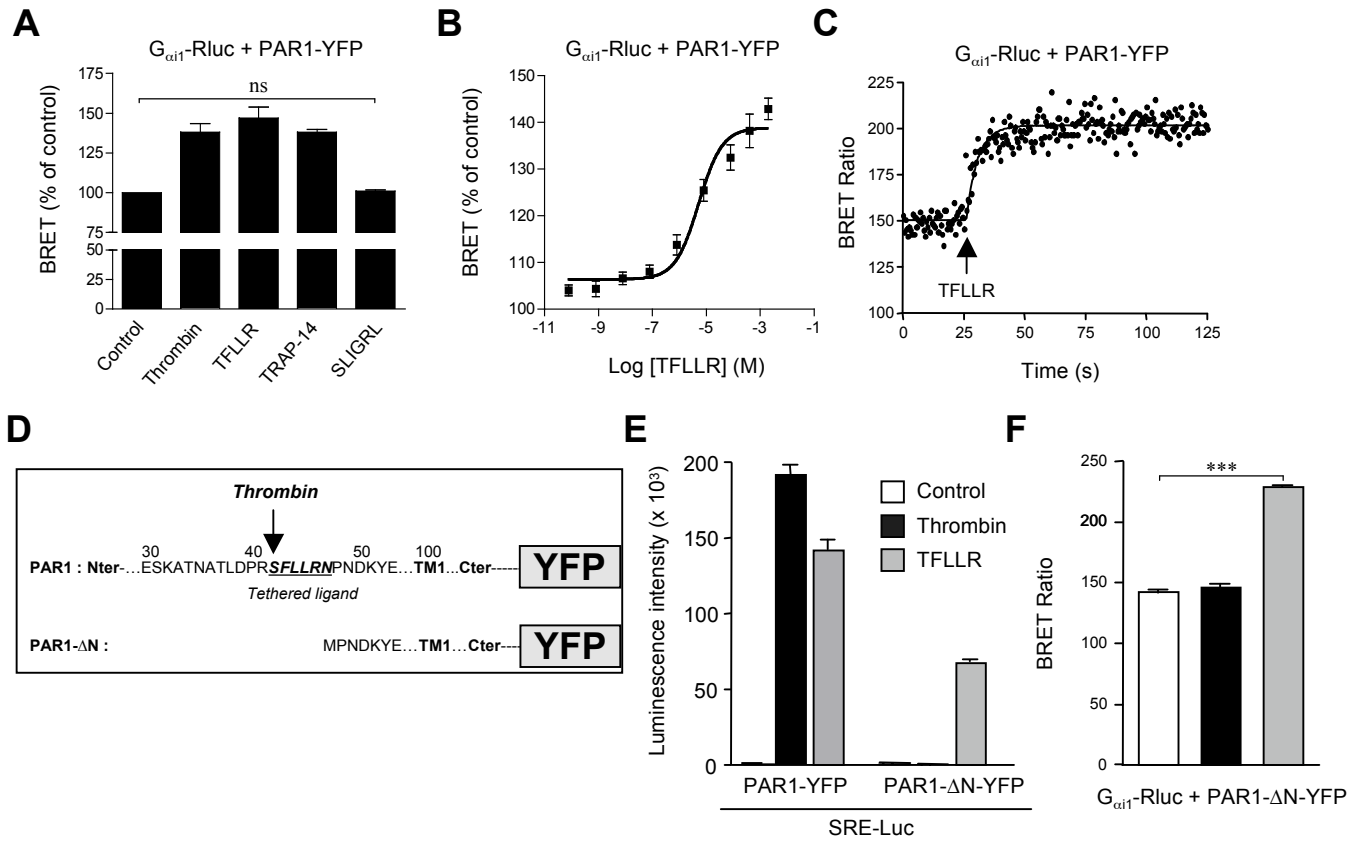
Figure 8

Figure 9

MOL #30304

Figure 10

Figure 11

MOL #30304

A

B

C

D